Published in final edited form as:
Science. 2013 January 18; 339(6117): 324–328. doi:10.1126/science.1231921.

GDE2 promotes neurogenesis by glycosylphosphatidylinositol-anchor cleavage of RECK

Sungjin Park[1,*], **Changhee Lee**[1,*], **Priyanka Sabharwal**[1], **Mei Zhang**[1], **Caren L. Freel Meyers**[2], and **Shanthini Sockanathan**[1,**]

[1]The Solomon Snyder Department of Neuroscience, The Johns Hopkins University, School of Medicine, PCTB1004, 725 N Wolfe Street, Baltimore, MD 21205, Phone: (410) 502-3084; Fax: (410) 614-8423

[2]Department of Pharmacology and Molecular Sciences, The Johns Hopkins University, School of Medicine, 725 N Wolfe Street, Baltimore, MD 21205

Abstract

The six-transmembrane protein glycerophosphodiester phosphodiesterase 2 (GDE2) induces spinal motor neuron differentiation by inhibiting Notch signaling in adjacent motor neuron progenitors. GDE2 function requires activity of its extracellular domain that shares homology with glycerophosphodiester phosphodiesterases (GDPD). GDPDs metabolize glycerophosphodiesters into glycerol-3-phosphate and corresponding alcohols but whether GDE2 inhibits Notch signaling by this mechanism is unclear. Here, we show that GDE2, unlike classical GDPDs, cleaves glycosylphosphatidylinositol (GPI)-anchors. GDE2 GDPD activity inactivates the Notch activator RECK by releasing it from the membrane by GPI-anchor cleavage. RECK release disinhibits ADAM protease-dependent shedding of the Notch ligand Delta-like 1 (Dll1) leading to Notch inactivation. This study identifies a previously unrecognized mechanism to initiate neurogenesis that involves GDE2 mediated surface cleavage of GPI-anchored targets to inhibit Dll1-Notch signaling.

The transition from cellular proliferation to differentiation is tightly controlled to ensure appropriate numbers of distinct cell types are formed, and to prevent the depletion or uncontrolled proliferation of progenitor cells. Glycerophosphodiester phosphodiesterase 2 (GDE2) is necessary and sufficient to induce differentiation of spinal motor neuron (MN) subtypes. GDE2 acts non cell-autonomously by inhibiting Notch signaling in neighboring Oligodendrocyte transcription factor 2 ($Olig2^{+}$)MN progenitors using extracellular glycerophosphodiester phosphodiesterase (GDPD) domain activity (1–4). Because Notch is activated by ligands Delta-like (Dll) and Jagged (Jag) expressed in adjacent cells, we tested whether GDE2 might target Dll1 and Jag1 function (3, 5). Jag1 and Dll1 are expressed in non-overlapping domains within the ventral spinal cord, and genetic ablation of either ligand causes domain-specific precocious neuronal differentiation (fig.S1A) (5–7). Spinal cords of mice lacking GDE2 (*Gde2*$^{-/-}$) showed a specific loss of MNs and V0 interneurons, no changes in the total number of V1 interneurons or V2 interneurons, but an increase in the ratio of V2a:V2b interneurons (Fig.1, A to I; 3). These domain-specific deficits correspond

**Author for correspondence:ssockan1@jhmi.edu.
*These authors contributed equally

Supplementary Materials
Materials and Methods
Figs S1–S11.
Table S1.
References (27– 34)

to regions of Dll1 expression and function, suggesting that GDE2 specifically targets Dll1, but not Jag1 activity (fig.S1A).

Dll1 is inactivated through cleavage and release of its extracellular domain (ECD) by the ADAM metalloprotease family (5). To determine if GDE2 GDPD activity promotes Dll1 shedding we coelectroporated plasmids expressing GDE2 and C-terminal Flag-tagged Dll1 (Dll1-Flag) into chick spinal cords and analyzed Dll1 processing by protein immunoblotting. Overexpression of Dll1-Flag generated full-length Dll1 and a processed 30kD C-terminal fragment (CTF) (Fig.1J). Overexpression of GDE2 and Dll1-Flag induced accumulation of a C-terminal 42kD Dll1 product (Dll1-42) that was not generated by coexpression of the two-pass transmembrane GDPD protein GDE1 (4, 8), or by catalytically inactive GDE2 GDPD mutants (GDE2.APML; 3) (Fig.1J). A corresponding N-terminal Dll1 ECD fragment was detected after overexpressing a double tagged version of Dll1 (Myc-Dll1-Flag) (fig.S2). Fluorescence-activated cell sorting (FACS) analysis of Dll1 expression showed decreased Dll1 surface expression in MNs when GDE2 was overexpressed in chick spinal cords and a corresponding increase of endogenous Dll1 surface expression in GFP^+ MNs purified from *HB9:GFP;Gde2*$^{-/-}$ animals (fig.S3; 9). Consistent with the Dll1-specific function of GDE2, no changes in Jag1 expression (Jag1FL) or processing (Jag1CTF) were detected in spinal cords overexpressing GDE2 or in spinal cords of *Gde2*$^{-/-}$ animals (Fig.1, J and K). These data indicate that GDE2 GDPD activity stimulates Dll1 processing, and decreases the availability of cell surface Dll1 in vivo. In addition to removing surface Dll1 for Notch receptor activation, the released Dll1 ECD is reported to inhibit Notch signaling by a dominant-negative activity (5); thus, Dll1 should function cooperatively with GDE2 to induce MN differentiation. Indeed, overexpression of GDE2 with Dll1 in chick spinal cords enhanced the ability of GDE2 to induce premature differentiation of ventricular zone (VZ) progenitors into $Isl2^+$ MNs (Fig.1, L to N).

GDE2 did not induce Dll1-42 accumulation when coexpressed with Dll1-Flag in heterologous human embryonic kidney (HEK) 293T cells; thus, GDE2-dependent processing of Dll1 is likely indirect (fig.S1B). Overexpression of ADAM10 and Dll1-Flag in chick spinal cords induced formation of Dll1-42 and decreased surface Dll1, suggesting that Dll1-42 may be generated through ADAM metalloprotease activity (figs.S3B and S4). Further, ADAM10 overexpressed in chick spinal cords effectively cleaved Dll1Δclv, which lacks a reported ADAM10 cleavage site mapped in vitro (10), suggesting that Dll1-42 may be generated by ADAM proteolytic activity through a separate cleavage site that is preferentially utilized in vivo (fig.S4). Thus, GDE2 GDPD activity appears to stimulate ADAM-dependent processing of Dll1 to Dll1-42, thereby inducing MN differentiation.

The GPI-anchored protein, Reversion-inducing Cysteine-rich protein with Kazal motifs (RECK), activates Notch signaling in cortical progenitors by directly inhibiting ADAM10-dependent Dll1 processing (11, 12). *RECK* mRNA is enriched in VZ cells and overlaps with GDE2 expression in newly differentiating MNs during neurogenesis (fig.S5, A and B). Depletion of *RECK* in spinal cords by two different sh*RNA*s (fig.S5, C and D) lowered Notch signaling as assayed by reduced expression of downstream Notch target genes *Hes5* and *Blbp* (5), and the induction of premature MN differentiation in the VZ (Fig.2, A to L). Moreover, loss of RECK specifically induced accumulation of Dll1-42 in spinal cords but did not alter Jag1 expression and processing to Jag1CTF (Fig.2M). These phenotypes are similar to those caused by GDE2 overexpression, and indicate that GDE2 GDPD activity may promote Dll1 shedding by inactivating RECK (1–3).

To determine how GDE2 GDPD activity might inactivate RECK, we tested if GDE2 exhibits classical GDPD phospholipase-D (PLD) catalysis in a coupled spectrophotometric assay of GDPD function (Fig.3, A and B) (13). Membrane fractions of HEK293T cells

transfected with control GDE1 showed GDPD activity when incubated with glycerophosphoserine (GPserine), or a cyclic glycerol-1,2-phosphate intermediate (cyG[1,2]P) that is not substrate-specific and formed by GDPD enzymes during their predicted 2-step catalytic mechanism (Fig.3, A and B; 14). However, GDE2 showed no GDPD activity in either case (Fig.3B). The GDPD domains of the six-transmembrane GDEs (GDE2, GDE3 and GDE6) are homologous to the catalytic X-domain of PI-PLC. GDE3, unlike GDE1, hydrolyzes GPinositol through a PLC-type cleavage mechanism (15, 16). Since exogenous bacterial PI-PLCs cleave and release GPI-linked proteins from membranes, we tested whether GDE2 GDPD activity inactivates RECK by GPI-anchor cleavage. We overexpressed GDE2 and RECK in HEK293T cells and assayed the culture medium for cleaved RECK ECD by protein immunoblotting. GDE2 and RECK co-expression released RECK into the medium, as does treatment with PI-PLC, whereas medium prepared from cells transfected with vector alone, GDE1 or catalytically inactive GDE2.APML contained little RECK (Fig.3, C and E). Repeated Triton X-114 extraction of medium from cells overexpressing GDE2 and RECK yielded RECK in hydrophilic fractions, ruling out potential medium contamination by membrane-bound RECK (Fig.3D; 17). Further, sequential expression of RECK and GDE2 released RECK into the medium (fig.S6), suggesting that GDE2 acts on surface GPI-anchored RECK and does not promote aberrant RECK discharge through disruption of RECK synthesis, modification or transport. Consistent with inactivation of RECK by GDE2 through cleavage of its GPI-anchor, endogenous RECK processing examined by Triton X-114 partitioning of cortical extracts showed reduced RECK release in *Gde2*$^{-/-}$ animals compared with that of WT littermates (fig.S7).

To date, two vertebrate GPI-anchored cleaving enzymes have been identified, GPI-PLD and the vertebrate homolog of Drosophila Notum (18, 19). Notum failed to release RECK into the medium of transfected HEK293T cells; while GPI-PLD led to effective RECK cleavage (fig.S8A). Analysis of surface biotinylated RECK in transfected HEK293T cells showed that GDE2 activity releases biotinylated RECK from the surface membrane into the medium; in contrast, GPI-PLD did not, suggesting that GPI-PLD cleavage of RECK is intracellular and occurs within the ER or Golgi (Fig.3F). Taken together, these observations indicate that GDE2 mediated release of RECK occurs on the cell surface and is independent from the function of known vertebrate GPI-anchor cleaving enzymes.

To define the mechanism of RECK release by GDE2, we radiolabeled transfected HEK293T cells and confirmed that the RECK ECD released into the medium by GDE2 expression contained components of the GPI-anchor such as [^{3}H] inositol or [^{3}H] ethanolamine, whereas a secreted version of RECK ECD (sRECK) that lacked the GPI anchor was poorly labeled under identical conditions (Fig.3G and fig.S8B; 20). Moreover, cells overexpressing RECK in which the GPI-anchor was replaced with the transmembrane domain from the non-GPI-anchored CD2 protein failed to produce RECK in the medium in the presence of GDE2 (fig.S9, A and B; 21, 22). These observations indicate that RECK release by GDE2 involves specific cleavage within the GPI-anchor, a concept supported by the ability of GDE2 to cleave other unrelated GPI-anchored proteins such as the glypicans GPC2 and GPC4 (fig.S10). PLD cleavage of the GPI-anchor would result in loss of a phosphate group from the phosphatidylinositol domain of released RECK when compared with PLC cleavage mechanisms (Fig.3G). Comparison of radiolabeled [^{32}P] incorporation between RECK ECD generated by GDE2 or GPI-PLD expression normalized to [^{3}H] inositol levels showed that RECK released by GDE2 contained higher ratios of [^{32}P]: [^{3}H] inositol than when cleaved by GPI-PLD (Table S1). This observation suggests that GDE2 release of RECK does not employ a similar mechanism to GPI-PLD. Bacterial PI-PLC cleavage of GPI linkages creates a unique stable 1,2 cyclic inositol phosphate ring (cyIno[1,2]P), that is recognized by antibodies to cross-reacting determinant (CRD) (23, 24). RECK ECD generated from GDE2

overexpression did not cross react with anti-CRD antibodies (fig.S8C), suggesting that GDE2 cleavage of GPI-anchors is different to that of bacterial PI-PLC; however, this observation is consistent with reports that mammalian PLC enzymes have different kinetics to bacterial PI-PLCs and fail to generate stable cyclic intermediates (25).

If GDE2 inactivates RECK to induce MN differentiation, then overexpression of RECK might overcome GDE2 inhibition and suppress GDE2-dependent induction of premature MN generation in the VZ. We used Cre-lox techniques to generate mosaic expression of GDE2 in $Olig2^+$ MN progenitors. This caused neighboring cells to differentiate into $Isl2^+$ MNs (3, 26). WT GPI-anchored RECK overexpressed with GDE2 effectively suppressed GDE2-dependent premature MN differentiation (Fig.4B and fig.S9, E and F). Overexpressed RECK-CD2 more effectively suppressed GDE2 induction of MN differentiation than did equivalent amounts of GPI-anchored RECK (Fig.4A and fig.S9, C and D), further indicating that GDE2 inactivates RECK to induce MN differentiation through cleavage of the GPI-anchor.

RECK ECD generated after GPI-anchor cleavage should be inactive and fail to maintain $Olig2^+$ MN progenitors through Notch activation. However, soluble versions of RECK that lack the GPI-anchor are active in other systems, suggesting that the activity of cleaved RECK is context dependent (11). Using similar Cre-lox approaches we compared the effects of WT RECK and sRECK to inhibit GDE2-dependent MN generation in electroporated chick spinal cords. Overexpression of WT RECK with GDE2 suppressed GDE2-dependent premature differentiation of MNs (Fig.4B and fig.S9F); in contrast, sRECK failed to suppress GDE2 activity (Fig.4B and fig.S9G). WT RECK was sufficient to prevent increased Dll1 shedding resulting from ablation of endogenous RECK by sh*RNAs*, whereas sRECK had no effect (Fig.4C). These observations suggest that RECK ECD fails to inhibit Dll1 shedding and imply that GDE2 GDPD-dependent cleavage of RECK clears active RECK from the membrane.

Our data suggest a model where GDE2 promotes MN differentiation by inactivating surface bound RECK through GPI-anchor cleavage, thus allowing ADAM protein function (fig.S11). GDE2 cleaves GPI-anchored proteins at the cell surface in multiple in vitro and in vivo contexts that are independent of known GPI-anchor cleaving enzymes. These observations support direct modes of cleavage, an activity shared by its family members GDE3 and GDE6 (fig.S9; 4); nevertheless, it remains possible that their function could involve stimulation of unidentified cleaving enzymes. GPI-anchored proteins are key regulators of signaling pathways that control diverse biological processes in the developing and adult organism (27, 28). Understanding how these pathways are regulated through GPI-anchor cleavage in normal and diseased states might be gained by further analysis of six-transmembrane GDE GDPD protein expression, transport and activity.

Supplementary Material

Refer to Web version on PubMed Central for supplementary material.

Acknowledgments

We thank P. Englund, M. Goulding, T.M Jessell and B. Novitch for antibodies; Dr J. Filmus for Notum plasmids; the Flow Cytometry and Cell Sorting Core Facility, Johns Hopkins Bloomberg School of Public Health; C. Cave III, A.L. Kolodkin, P.F. Worley and Y.Yan for comments on the manuscript, and lab members for discussions. This work was funded by NINDS RO1NS046336.

References and notes

1. Rao M, Sockanathan S. Transmembrane protein GDE2 induces MN differentiation in vivo. Science. 2005; 309:2212–2215. [PubMed: 16195461]
2. Yan Y, Sabharwal P, Rao M, Sockanathan S. The antioxidant Prdx1 controls MN differentiation by thiol-redox dependent activation of GDE2. Cell. 2009; 138:1209–1221. [PubMed: 19766572]
3. Sabharwal P, Lee C, Park S, Rao M, Sockanathan S. GDE2 regulates subtype specific MN generation through inhibition of Notch signaling. Neuron. 2011; 71:1058–1070. [PubMed: 21943603]
4. Yanaka N. Mammalian glycerophosphodiester phosphodiesterases. Biosci. Biotechnol. Biochem. 2007; 71:1811–1818. [PubMed: 17690467]
5. D'Souza B, Meloty-Kapella L, Weinmaster G. Canonical and non-canonical Notch ligands. Curr. Top. Dev. Biol. 2010; 92:73–129. [PubMed: 20816393]
6. Lindsell CE, Boulter J, diSibio G, Gossler A, Weinmaster G. Expression patterns of Jagged, Delta1, Notch1, Notch2, and Notch3 genes identify ligand-receptor pairs that may function in neural development. Mol. and Cell. Neurosci. 1996; 8:14–27.
7. Marklund U, et al. Domain-specific control of neurogenesis achieved through patterned regulation of Notch ligand expression. Development. 2010; 137:437–445. [PubMed: 20081190]
8. Zheng B, Berrie CP, Corda D, Farquhar MG. GDE1/MIR16 is a glycerophosphoinositol phosphodiesterase regulated by stimulation of G protein-coupled receptors. Proc Natl Acad Sci U.S.A. 2003; 100:1745–1750. [PubMed: 12576545]
9. Wichterle H, Lieberam I, Porter JA, Jessell TM. Directed differentiation of embryonic stem cells into MNs. Cell. 2002; 110:385–397. [PubMed: 12176325]
10. Six E, et al. The Notch ligand Delta1 is sequentially cleaved by an ADAM protease and gamma-secretase. Proc Natl Acad Sci U S A. 2003; 100:7638–7643. [PubMed: 12794186]
11. Muraguchi T, et al. RECK modulates Notch signaling during cortical neurogenesis by regulating ADAM10 activity. Nat. Neurosci. 2007; 10:838–845. [PubMed: 17558399]
12. Rhee JS, Coussens LM. RECKing MMP function: implications for cancer development. Trends Cell Biol. 2002; 12:209–211. [PubMed: 12062160]
13. Ohshima N, et al. Escherichia coli cytosolic glycerophosphodiester phosphodiesterase (UgpQ) requires Mg2+, Co2+, or Mn2+ for its enzyme activity. J. Bacteriol. 2008; 190:1219–1223. [PubMed: 18083802]
14. Shi L, Liu JF, An XM, Liang DC. Crystal structure of glycerophosphodiester phosphodiesterase (GDPD) from Thermoanaerobacter tengcongensis, a metal ion-dependent enzyme: insight into the catalytic mechanism. Proteins. 2008; 72:280–288. [PubMed: 18214974]
15. Corda D, et al. The developmentally regulated osteoblast phosphodiesterase GDE3 is glycerophosphoinositol-specific and modulates cell growth. J. Biol. Chem. 2009; 284:24848–24856. [PubMed: 19596859]
16. Rebecchi MJ, Pentyala SN. Structure, function, and control of phosphoinositide-specific phospholipase C. Physiol. Rev. 2000; 80:1291–1335. [PubMed: 11015615]
17. Doering TL, Englund PT, Hart GW. Detection of glycophospholipid anchors on proteins. Curr. Protoc. Protein Sci. 2001; Chap. 12(Unit 12.5)
18. Tsujioka H, Misumi Y, Takami N, Ikehara Y. Posttranslational modification of glycosylphosphatidylinositol (GPI)-specific phospholipase D and its activity in cleavage of GPI anchors. Biochem Biophys Res Commun. 1998; 251:737–743. [PubMed: 9790979]
19. Traister A, Shi W, Filmus J. Mammalian Notum induces the release of glypicans and other GPI-anchored proteins from the cell surface. Biochem J. 2008; 410:503–511. [PubMed: 17967162]
20. Paulick MG, Bertozzi CR. The glycosylphosphatidylinositol anchor: a complex membrane-anchoring structure for proteins. Biochemistry. 2008; 47:6991–7000. [PubMed: 18557633]
21. Gallet A, Staccini-Lavenant L, Thérond PP. Cellular trafficking of the glypican Dally-like is required for full-strength Hedgehog signaling and wingless transcytosis. Dev. Cell. 2008; 14:712–725. [PubMed: 18477454]

22. Yan D, Wu Y, Feng Y, Lin SC, Lin X. The core protein of glypican Dally-like determines its biphasic activity in wingless morphogen signaling. Dev. Cell. 2009; 17:470–481. [PubMed: 19853561]

23. Bangs JD, Hereld D, Krakow JL, Hart GW, Englund PT. Rapid processing of the carboxyl terminus of a trypanosome variant surface glycoprotein. Proc. Proc. Natl. Acad. Sci. U.S.A. 1985; 82:3207–3211. [PubMed: 3858818]

24. Zamze SE, Ferguson MA, Collins R, Dwek RA, Rademacher TW. Characterization of the cross-reacting determinant (CRD) of the glycosylphosphatidylinositol membrane anchor of Trypanosoma brucei variant surface glycoprotein. Eur. J. Biochem. 1988; 176:527–534. [PubMed: 2458923]

25. Heinz DW, Essen L, Williams RL. Structural and Mechanistic Comparison of Prokaryotic and Eukaryotic Phosphoinositide-specific Phospholipases C. J. Mol. Biol. 1998; 275:635–650. [PubMed: 9466937]

26. Zhuang B, Su YS, Sockanathan S. FARP1 promotes the dendritic growth of spinal MN subtypes through transmembrane Semaphorin6A and PlexinA4 signaling. Neuron. 2009; 61:359–372. [PubMed: 19217374]

27. Yan D, Lin X. Shaping morphogen gradients by proteoglycans. Cold Spring Harb Perspect Biol. 2009; 1:a002493. [PubMed: 20066107]

28. Fico A, Maina F, Dono R. Fine-tuning of cell signaling by glypicans. Cell Mol. Life Sci. 2011; 68:923–929. [PubMed: 18087675]

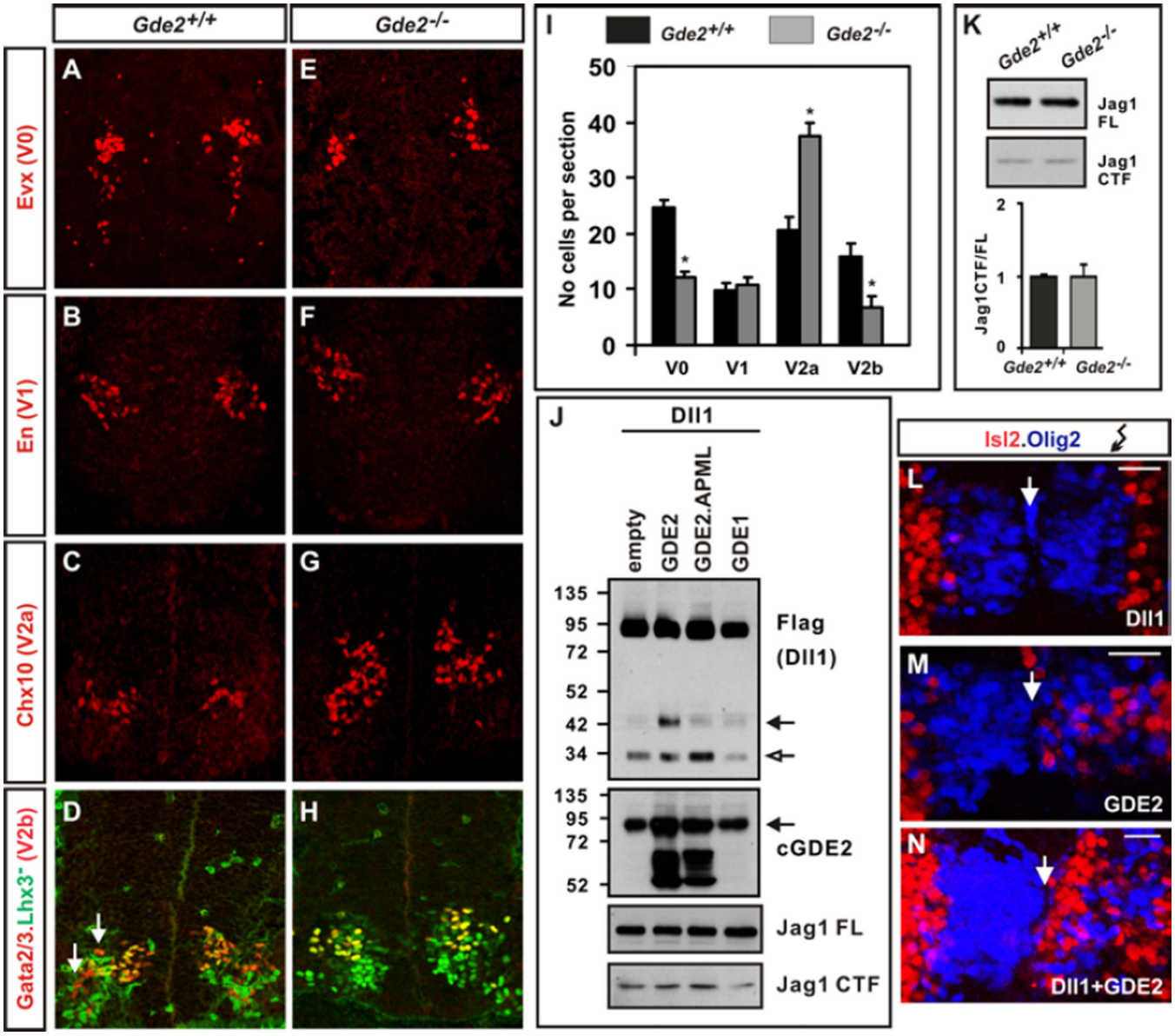

Figure 1. Stimulation of Dll1 shedding by GDE2

(A–H) Coronal sections of E13.5 mouse spinal cords. Arrows mark V2b interneurons (red). (I) Graph quantifying interneuron numbers in WT and *Gde2*$^{-/-}$ mutants; mean ± s.e.m, n= 4, two-tailed t-test: V0 *p= 0.0016; V1 p= 0.4778; V2a *p= 0.0028, V2b *p= 0.0088 (J) Western blots of extracts of chick spinal cords electroporated with Dll1-Flag plasmid; open arrow = 30kD Dll1 C-terminal fragment, black arrow = C-terminal 42kD Dll1 product (Dll1-42). Arrow (GDE2) = endogenous glycosylated GDE2, lower bands are hypoglycosylated GDE2. (K) Western blot of Jag1 processing (FL= full length; CTF= C-terminal fragment) and quantification of Jag1 CTF/FL ratios from E12.5 embryonic spinal cord extracts. (L–N) Close up of electroporated chick spinal cords (right) shows increased Isl2^{+} MNs (red) when Dll1 is coelecroporated with GDE2. Arrow = midline. Scale bar = 20μm.

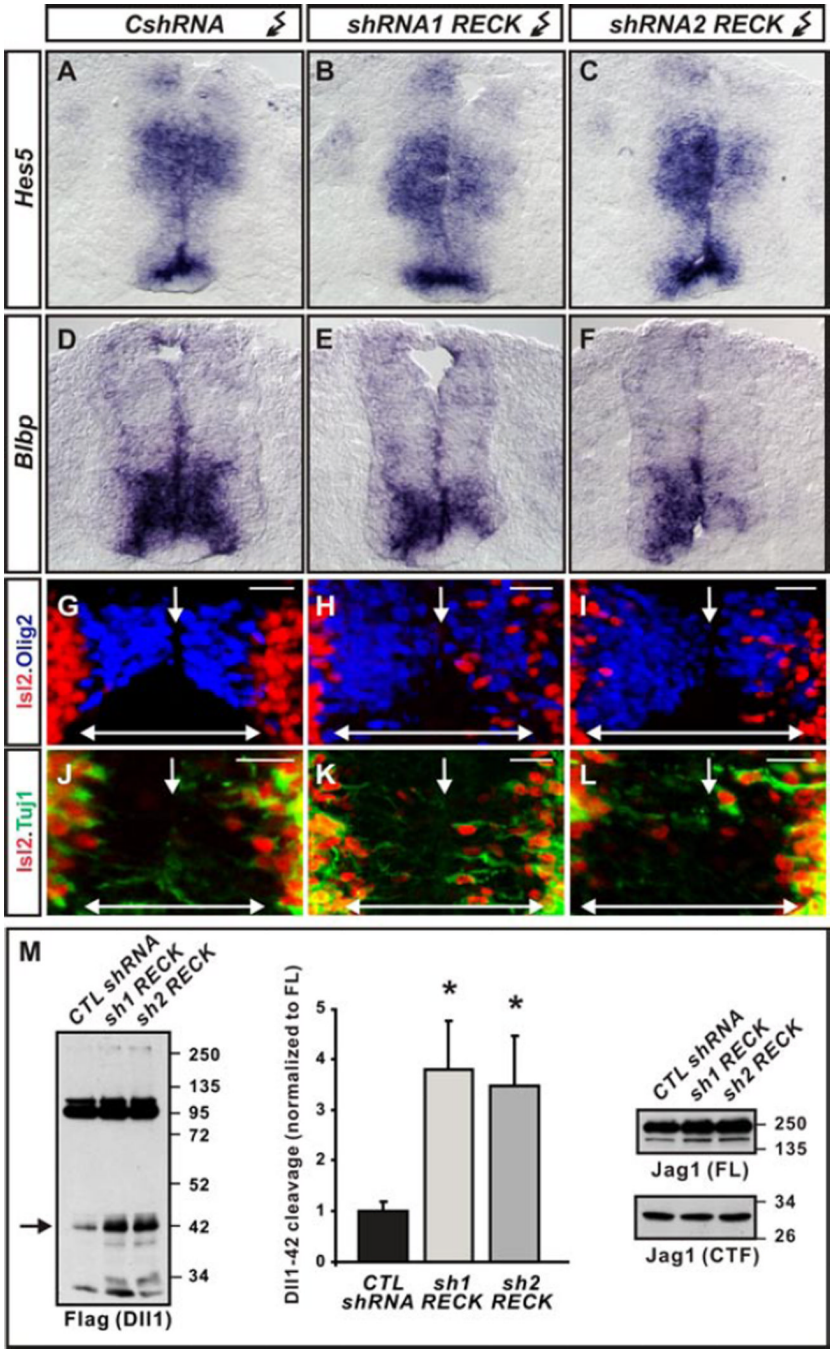

Figure 2. Effects of RECK ablation

(A–F) Notch target gene mRNAs are reduced in HH st19/20 chick spinal cords electroporated with *RECK shRNAs* but not control *CshRNAs*. (G–L) Olig2 expression (blue) demarcates VZ of chick spinal cords electroporated (right) with control and *RECK shRNAs*, showing Isl2^{+} MNs (red) that express neuronal Tuj1 (green) when RECK is knocked-down. Arrow = midline; doubleheaded arrow = VZ. Scale bar = 20μm. (M) Western blots of chick spinal cords electroporated with Dll1-Flag plasmid and *RECK shRNAs* show RECK knockdown stimulates Dll1-42 production (arrow) but Jag1 expression and processing is unchanged. Graph quantifying Dll1-42 cleavage from

Westerns; mean ± s.e.m. Two-tailed t-test, n=4, *sh1RECK* *p= 0.0066 *sh2RECK* *p=0.0175.

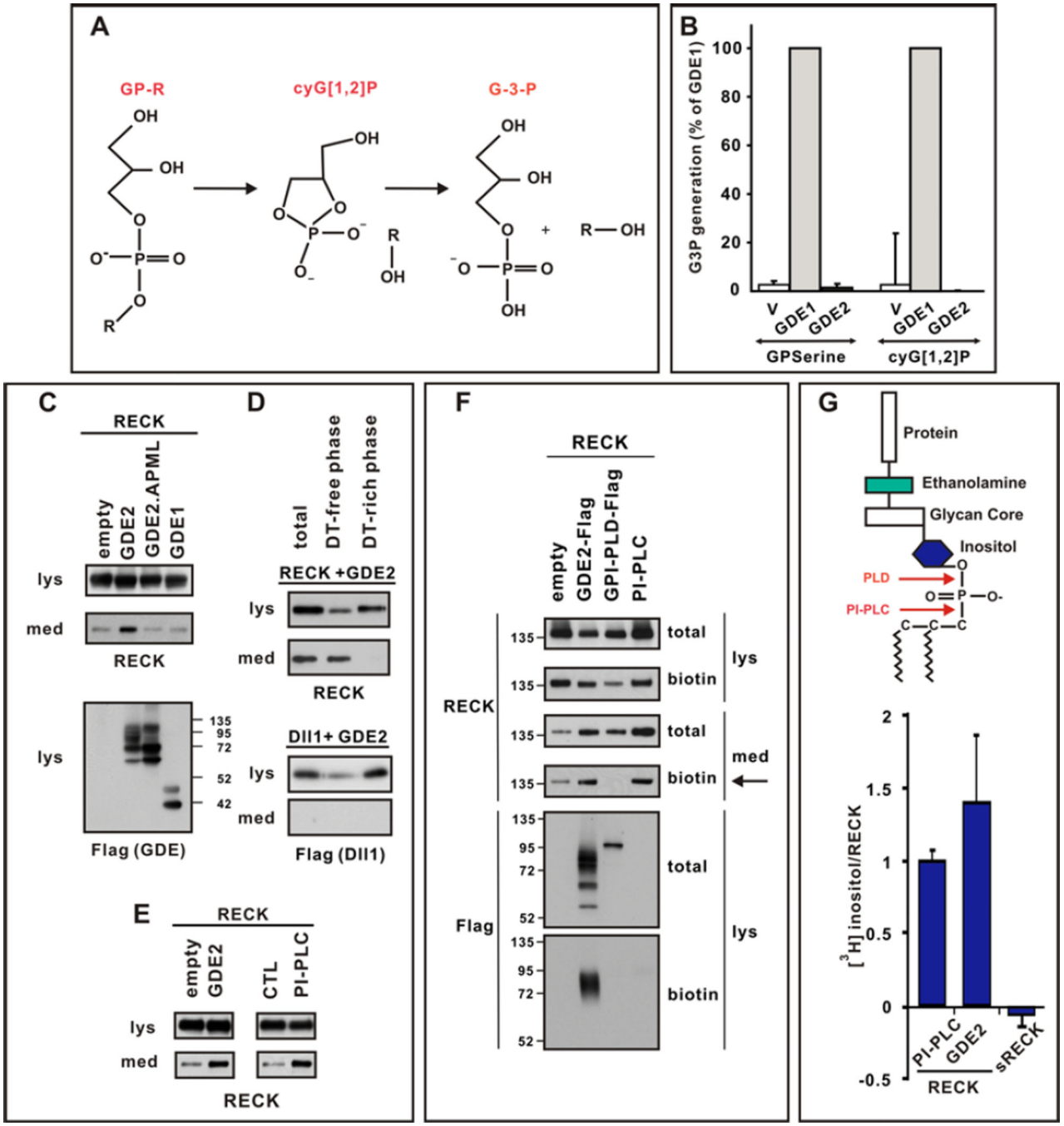

Figure 3. GDE2 cleaves RECK within the GPI-anchor

(A) Schematic of 2-step GDPD catalysis. (B) Graph quantifying in vitro GDPD assay in transfected HEK293T cells using glycerophosphoserine (GPserine) and synthetic cyclic glycerol[1,2] phosphate intermediate. (C–E) Western blots of transfected HEK293T cell lysates (lys) and medium (med). (C) RECK is detected in the medium when catalytically active GDE2 is present. (D) After sequential Triton X-114 extraction cleaved RECK is observed in the Detergent (DT)-free hydrophilic phase, while Dll1, which is not cleaved by GDE2, is retained in DT-rich hydrophobic phase of the lysate. (E) RECK ECD is generated by GDE2 or PI-PLC activities. (F) Western blot of lysates (lys) and medium (med) of HEK293T cells transfected with RECK and C-terminal Flag tagged GDE2 or GPI-PLD.

Surface RECK is labeled by biotin. GDE2 but not GPI-PLD releases surface biotinylated RECK into the medium (arrow). Both GDE2 and GPI-PLD are visualized by Flag antibodies but only GDE2 is labeled by biotin indicating GDE2 is localized to the cell surface. PI-PLC was added to intact cells and serves as a positive control. (G) Schematic of GPI-anchor. Graph quantifying amount of radiolabel incorporated into RECK or secreted (s) RECK when GDE2 or PI-PLC is present. Mean ± s.e.m. n=4–12.

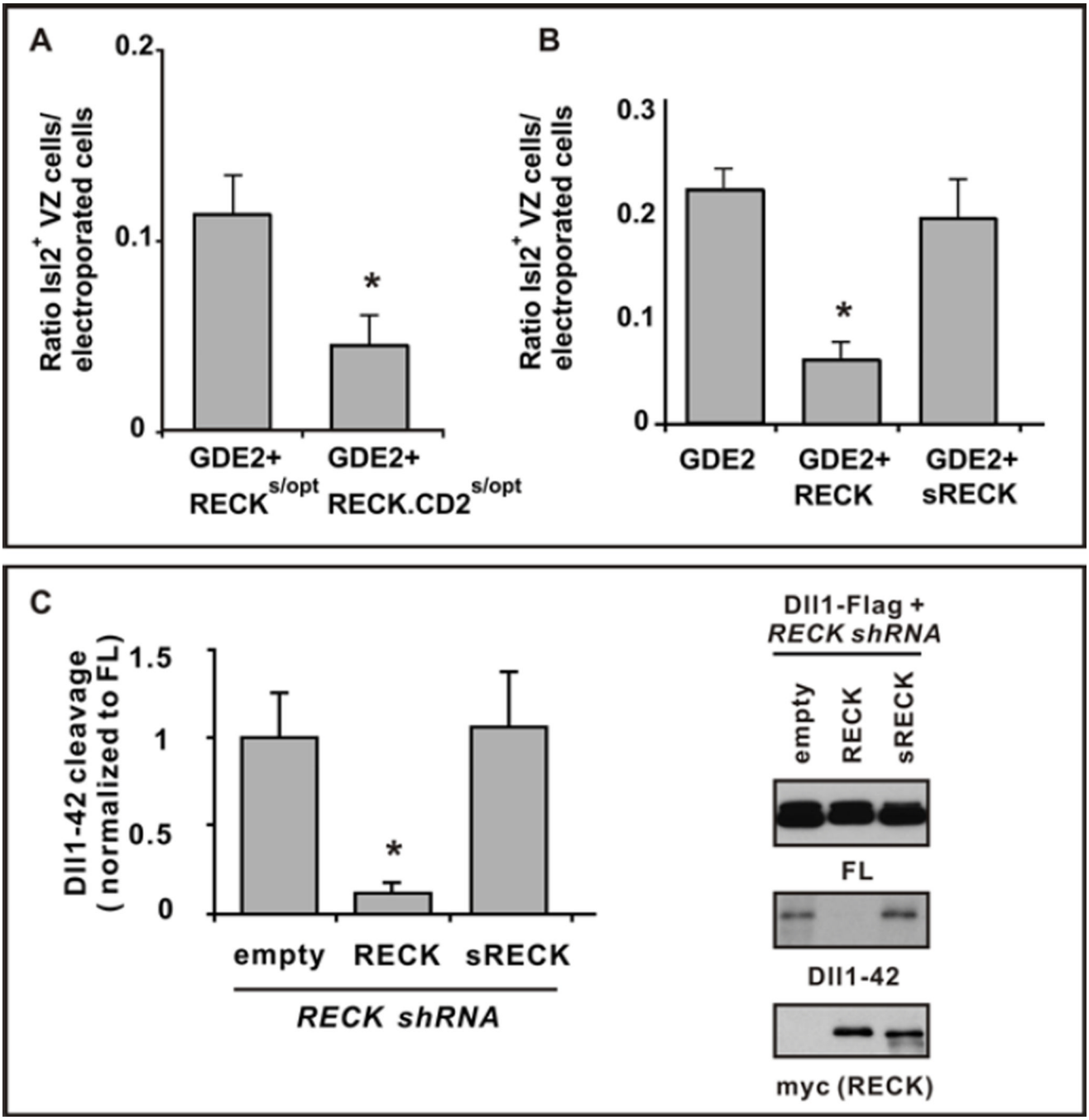

Figure 4. GDE2 inactivates RECK by GPI-anchor cleavage

(A, B) Graphs quantifying ratio of ectopic Isl2^{+} VZ MNs normalized to the number of transfected GDE2 cells. Mean ± s.e.m., two-tailed t-test, (A) Suboptimal levels of plasmids expressing RECK$^{s/opt}$ or RECK-CD2 $^{s/opt}$ were coelectroporated with GDE2. RECK-CD2 was more effective than RECK in suppressing GDE2 dependent MN generation, *p= 0.0306 (n=5); (B) Plasmids expressing RECK or sRECK were coelectroporated with GDE2; RECK effectively suppressed GDE2 function but sRECK did not, *p= 5.59×10^{-5} (n=8–10) compared with GDE2. (C) Western blot of extracts of chick spinal cords electroporated with Dll1-Flag and *RECK shRNA* targeting 3' UTR to detect full-length (FL) and processed Dll1-42. The phenotype is rescued by exogenous plasmids expressing WT RECK ORF but

not sRECK. Densitometric quantification of Dll1-42, mean ± s.e.m., n=4. Two-tailed t-test, *p=0.013 compared with empty.